Review Article   **Open Access**

A Survey of Computer-aided Detection of Breast Cancer with Mammography

Yanfeng Li, Houjin Chen*, Lin Cao and Jinyuan Ma

School of Electronic and Information Engineering, Beijing Jiaotong University, Beijing, China

Abstract

Computer-aided detection (CAD) systems can be served as a second view for radiologist. An overview of recent development in CAD methods are presented in this paper. Abnormalities detection, abnormalities classification and content-based image retrieval (CBIR) are briefly reviewed. For the abnormalities detection, micro-calcification detection, mass detection and multi-view based detection are introduced. For the abnormalities classification, micro-calcification classification and mass classification are given.

Introduction

Breast cancer is one of the common malignant tumors among women. According to the statistics, the number of new breast cancer for the women worldwide is about 1.67 million in 2012. This high morbidity accounts for about 25% in all cancers [1]. If breast cancer can be early detected, it is one of the most treatable malignancies [2]. From 1990s, the mortality of breast cancer has an obvious decrease in developed countries, such as in Europe and America [3,4]. Different imaging modalities are under different theories and show different characteristics in breast cancer detection. The mammography is one of the most widely used methods for breast cancer screening [5]. When taken a mammogram, the breast needs to be compressed. In screening mammography, two breasts are imaged and two different views are taken for each breast. The two views are cranio-caudal (CC) and mediolateral-oblique (MLO). An example for the four view mammograms is shown in Figure 1. The CC view is taken from a top view. Only few mammograms show the pectoral muscle. The MLO view is taken from an oblique view. The pectoral muscle is depicted obliquely and stretches down to the level of the nipple or further down. The shape of the muscle should be curve or bulge outward.

Computer-aided detection (CAD) systems employ image processing technique and pattern recognition theory to detect and classify abnormalities in mammograms, which can provide an objective view to the radiologist [6]. The abnormalities in mammograms include micro-calcifications (MCs), masses, architectural distortion, and asymmetry. In the past several years, many related techniques for abnormalities detection and classification have been studied. The aim of this paper is to provide an overview of some CAD methods. The rest of this paper is organized as follows. In Section II, abnormalities detection methods are given. In Section III, abnormalities classification methods are introduced. In Section IV, content-based image retrieval (CBIR) in mammogram is briefly reviewed. The discussions are given in Section V, and conclusions are given in Section VI.

Abnormality Detection

MCs detection

MCs are tiny deposits of calcium that appear as small bright spots in mammograms. Extensive researches have been conducted for MCs detection.

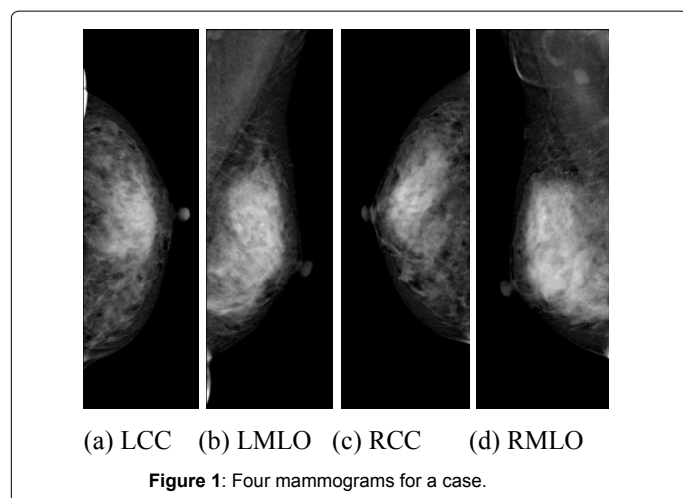Nakayama et al. [7] first decomposed the mammogram by filter bank. Then regions of interest (ROIs) were selected from the image. Eight features were extracted for each ROI. Finally the Bayes discriminant function was employed for distinguishing MC ROIs from normal ROIs. Kavitha et al. [8] presented an approach using filter bank, DCT and Bayesian classifier. The author applied the method to 40 mammograms and 99% detection accuracy was reported. Halkiotis et al. [9] combined mathematical morphology and artificial neural network (ANN) for MC detection. Bhattacharya et al. [10] put forward a method based on wavelet transform, top-hat transformation and fuzzy c-means clustering to detect MC. A multi-stage detection system was given in Pal et al. [11]. First a back-propagation neural network was used to find the candidate calcified regions. Then the network output was cleaned using connected component analysis and an algorithm for removing thin elongated structures. Finally, a measure of local density was used for a final classification. Oh et al. [12] first segmented the breast region using grey level co-occurrence matrix (GLCM). Then, foveal method was used to extract candidate of MC. Finally, false positive (FP) MCs were removed using a set of 8 features. Peng et al. [13] employed stochastic resonance (SR) noise to detect MCs. Mohanalin et al. [14] presented a detection method using a type II fuzzy index. Tested on 247 mammograms, the author reported a true positive (TP) rate is 96.55% with 0.4 FPs per image. Harirchi et al. [15] gave a two-level system for MC detection in mammograms. In the first step, six features consisting of four wavelet and two gray level features were used as the inputs to a multilayer neural network classifier to detect candidate MC pixels. Then, 25 features from candidate MCs were extracted and geometric linear discriminant analysis (GLDA) was used to reduce the features to 10. Finally, diverse Adaboost support vector machine (SVM) was used as second level classifier. Oliver et al. [16] detected the MCs based on extracting local features for characterizing the morphology of the MCs. The developed approach automatically learns and selects the most salient features. Then a boosted classifier was used to detect individual MCs. Zhang et al. [17] first enhanced the MCs using well-designed filter. Then the subspace learning algorithm was used for feature selection. Finally a twin support vector machine

(a) LCC   (b) LMLO   (c) RCC   (d) RMLO

Figure 1: Four mammograms for a case.

(TWSVM) was developed for classification. Recently, Zhang et al. [18] presented a method based on a morphological image processing and wavelet transform. Zhang et al. [19] gave a method using mathematical morphology and SVM. The author reported a detection rate of 94.85% at 0.53 FPs/I.

Mass detection

The general procedure for mass detection has three steps. First, the suspicious regions are detected. Then the shape and texture features of the region are extracted. Finally FP regions are removed based on the extracted features.

Petrosian et al. [20] used the texture features computed from GLCM to distinguish between mass and non-mass regions. Tested on a small database, a difference in the training and testing results was found. Petrick et al. [21] obtained potential masses using an adaptive density-weighted contrast enhancement (DWCE) filter and Laplacian-Gaussian (LG) edge detection. Then morphological features were extracted and input to a classifier to differentiate normal ROIs and mass ROIs. Campanini et al. [22] employed wavelet decomposition and SVM to detect masses in mammograms. The multi-resolution over-complete wavelet representation was first performed to the image. Then three expert systems were obtained under different SVM classifier. The final result was achieved by majority voting among the three systems. The author reported a detection rate of 80% with 1.1 FPs/I. Cascio et al. [23] first used an edge-based algorithm to segment the boundary of a ROI. Then geometrical features and shape features were extracted. Finally a neural network was trained for recognizing true mass. The author reported a detection rate of 82% with 2.8 FPs/I under 3762 mammograms. Pereira et al. [24] used sixteen texture features to represent a ROI. Then nonparametric KNN classifier was trained to discriminant normal ROIs from abnormal ROIs. Guo et al. [25] compared five fractal dimension (FD) estimation methods in describing mass ROIs and normal ROIs. The author reported that FD of mass ROI was statistically significantly lower than that of normal ROIs for all five methods. Ke et al. [26] first employed bilateral analysis to detect mass candidate. Then FD and two-dimensional entropy were extracted from the ROI. Finally a SVM classifier was trained. Tested on 106 mammograms, the author reported a detection rate of 85.11% at 1.44 FPs/I. Giordano et al. [27] employed a 2D Haar wavelet transform and region-based segmentation for mass detection. Hussain et al. [28] used multi-scale Weber local descriptor (MSWLD) and SVM for differentiating normal ROIs and mass ROIs. The author reported the

area under the receiver operating characteristics (ROC) curve is 0.988 for 512 ROIs. Gargouri et al. [29] proposed a new local pattern model named gray level and local difference (GLLD) to represent a ROI. Using 1000 ROIs from Digital Database for Screening Mammography (DDSM) database, the author reported the area under the ROC curve is 0.95. Nascimento et al. [30] presented a system using a polynomial classifier and wavelet coefficients to differentiate normal from abnormal tissues. Tai et al. [31] put forward a system using local and discrete texture features for mammographic mass detection.

Multi-view detection

For interpreting the mammogram, a radiologist normally compare four mammograms of a case. When a suspicious region is found in LCC view, the corresponding regions in the LMLO and RCC are checked. If the region in LMLO is also suspicious, the likelihood of this region being abnormal is increased. If the region in RCC is normal tissue, the likelihood of this region being abnormal is also increased. Combing different projection views of the same breast called ipsilateral analysis. Combing the same projection view of the left breast and the right breast is called bilateral analysis. Methods combining information from multiple mammographic views simulate the radiologist interpreting, which may improve the CAD performance using single view. A number of abnormal detection methods using multiple views were also studied.

Sun et al. [32] presented an ipsilateral multi-view CAD scheme for mass detection. Concurrent analysis was first developed for CC-MLO matching. Then a supervised ANN was employed as a classifier. Sahiner et al. [33] gave an MC detection scheme combining the CC view and the MLO view. Both the features of the CC-MLO pair and that of the candidate in the single-view were classified. The final detection result is the combination of these two classifiers. The author reported that the highest mammogram-based sensitivity by the CC-MLO pair classifier was 69%. The single-view classifier had a maximum mammogram-based sensitivity of 93% with a higher FPs. The fusion method got a better performance compared with the CC-MLO pair classifier and the single-view classifier. Engeland et al. [34] built a cascaded multiple-classifier system for mass detection. First the pixel level features were extracted and classified. Then the suspicious pixel was located and segmented. Region level features were extracted and input to another classifier. Finally, regions in different views were linked and two-view features were extracted. The final output is the third classifier with two-view features as input. The results showed that the lesion based detection performance was improved compared with the single view CAD. However, case based sensitivity did not improve. An FP reduction method based on bilateral analysis was presented [35]. GLCM-based texture features and morphological features were extracted from the suspicious ROI and its corresponding ROI on the contralateral mammogram. Then bilateral features were computed. Linear discriminant analysis (LDA) classifiers were trained for unilateral features and the bilateral features, respectively. The final result was the third classifier with unilateral-LDA and bilateral-LDA as inputs. Velikova et al. [36] employed a Bayesian network to model the relationship between the CC view and the MLO view. Li et al. [37] developed a CC-MLO MC detection system based on spatial matching and feature matching. Samulski et al. [38] presented a multi-view CAD system in order to optimize the case-based detection performance. After the suspicious ROIs in each view were found. Geometry-based matching, features in single view and the malignancy score for the ROI were employed to extract the similarity feature. Then a correspondence classifier was trained using the similarity feature. The final result was the combination of two two-view classifiers. The author reported a

significant increase of case-based detection performance. Tanner et al. [39] compared the performance of several common methods to define the search region for matching masses in CC and MLO mammograms. Ericeira et al. [40] first detected asymmetric ROIs in one mammogram based on bilateral analysis. Then the asymmetric ROIs were classified as normal or mass based on variogram. Li et al. [41] used the bilateral similarity analysis to reduce the FPs. Tested on a set of 332 mammograms, the methods shows a 34% FP reduction compared with the single-view CAD, with the detection sensitivity at 85%.

The aforementioned methods combine two mammograms to improve the detection performance. Wei et al. [42] presented a four-view CAD system. The CAD system consists of single-view detection, two-view analysis and bilateral analysis. The author reported the performance of the four-view CAD system is higher than the other three systems.

Abnormality Classification

MCs classification

Benign and malignant MCs are shown in Figure 2. Singh et al. [43] first segmented the ROI by edge detection and morphological operations. Then shape, texture and statistical features were extracted. Finally a SVM classifier was trained to classify MC clusters as either benign or malignant. Karahaliou et al. [44] tested the performance of texture features extracted from the tissue surrounding MCs. The author reported the best classification accuracy is 89%. Verma et al. [45] used 14 features to represent the ROI. Then a neural-genetic algorithm was proposed for feature selection. Geetha et al. [46] used GLCM to extract the Haralick features. Then two feature selection methods Genetic Algorithm (GA) and New Particle Swarm Optimization (NPSO) algorithms were employed. Wei et al. [47] presented a MC classification scheme assisted by content-based mammogram retrieval. Chen et al. [48] first analyzed the connectivity and topology of the MCs. Then graph theoretical features were extracted. Recently, Raghavendra et al. [49] employed Gabor wavelet and locality sensitive discriminant analysis (LSDA) to classify normal, benign and malignant abnormalities.

Mass classification

Based on the extracted features, mass classification can be divided into shape feature-based method and texture feature-based method. A precise mass contour segmentation is a preprocessing for shape-based classification. However, the texture-based classifications are more robust to the mass contour segmentation.

Shape-based classification: Benign masses are usually round or oval and possess well-defined edges. Malignant masses are typically spiculated and possess ill-defined edges. Benign masses and malignant masses are shown in Figure 3. Rangayyan et al. [50] proposed an edge acutance feature to describe the gray transition of the contour pixels. Then masses were classified as benign or malignant combining the acutance, compactness and the Fourier descriptor. Later, Rangayyan et al. [51] gave another mass classification method. First, the mass contour was modeled by the polygonal. Then two new features concavity fractions and spiculation index were computed. Finally, the classification performance using different combinations of concavity fractions, spiculation index and compactness were tested. Fractal dimension (FD) shows good performance in characterizing the shape complexity. Thus the performance of the FD in mass classification was tested [52]. In Rangayyan and Nguyen [52], four methods to compute the FD were given. This method was tested to a dataset of 111 breast

masses. For FD, the area under the ROC curve is 0.89. For computing shape-based features, the mass contours should be known. In these three methods, manually segmentation was employed to get the mass contours. Liu et al. [53] gave an automated mass segmentation method. Then several shape-based features were compared for mass classification. 292 images from the DDSM database were used for experiments. The method achieved an accuracy of 86.6% with mutual information based feature selection and SVM classifier.

Texture-based classification: Mudigonda et al. [54] extracted features from the GLCM to implement the mass classification. The GLCM features were extracted from both the whole mass region and the ribbon width across the mass contour. A total of 54 images were used to test the result. The author reported the better result is obtained using GCLM-based features computed from the ribbon. Other texture features includes independent component analysis (ICA) [55], wavelet transform coefficient [56], Curvelet transform coefficient [57], Contourlet transform coefficient [58] and Krawtchouk moment [59]. Texture descriptors show good performance in many classification tasks. Thus local ternary pattern (LTP), local phase quantization (LPQ) [60] and texton [61] were employed to classify a mass as malignant or benign.
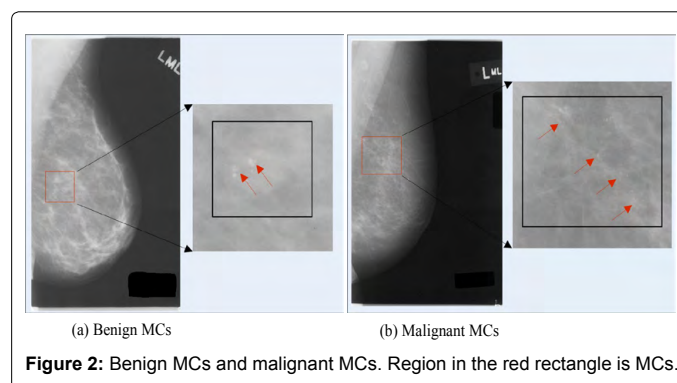

(a) Benign MCs   (b) Malignant MCs

Figure 2: Benign MCs and malignant MCs. Region in the red rectangle is MCs.

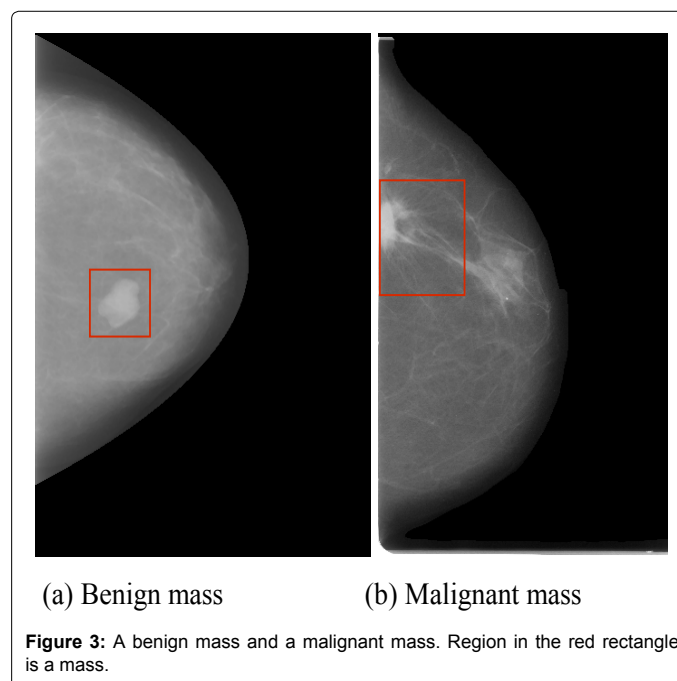(a) Benign mass   (b) Malignant mass

Figure 3: A benign mass and a malignant mass. Region in the red rectangle is a mass.

Recently, a combination of shape features and texture features were tested. Mu et al. [62] evaluated a set of 22 features including 8 shape features and 14 texture features. Using selected combinations of these 22 features, the classification performance was improved. Rouhi et al. [63] extracted intensity, texture, and shape features from a segmented tumor. Then the GA method was used to select features and ANN was used for classification.

Content-Based Image Retrieval (CBIR) in Mammography

CBIR is to choose images from a database such that the retrieved images are most relevant or similar to the query image. From the retrieval mammograms, the radiologist can get more comprehensive information. The most important issue in CBIR is similarity definition between two images. For this topic, a number of methods were studied.

Wei et al. [64] gave a calcification retrieval method. Gabor filtering was used to extract textural features as the similarity. In Wei et al. [65], a supervised learning approach was employed to retrieve mammograms. They defined the most meaningful measure as the one that matches the perception of the radiologist's interpretation. Alto et al. [66] first segmented the mass contour. Then the shape, edge sharpness and texture features were employed to retrieve benign masses and malignant masses. A hierarchical correlation approach was presented to retrieve masses and normal tissues in Wei et al. [67]. Siyahjani et al. [68] put forward a retrieval method for masses and normal tissues. In his method, multi-level wavelet transforms were applied to the ROI. Then the GLCM was computed for each sub-band. The texture features extracted from the GLCM were used to compute the similarity between different images. Georgia et al. [69] compared several similarities in masses and normal tissues retrieval. These similarities included joint entropy, conditional entropy, mutual information, normalized mutual information, average Kullback-Leibler divergence (KLD), maximum KLD, Jensen divergence and arithmetic-geometric mean divergence. The author reported that the mutual information and KLD are better. A preliminary study of multi-instance learning (MIL) was given for mass retrieval in Lu et al. [70]. Liu et al. [71] employed Anchor Graph Hashing (AGH) to represent a ROI. Then the Hamming distance of AGH was used to retrieve mass and normal tissues. A good retrieval performance was shown in their results. Later, Li et al. [72] gave a modification of AGH. As the original AGH representation did not consider pathological rele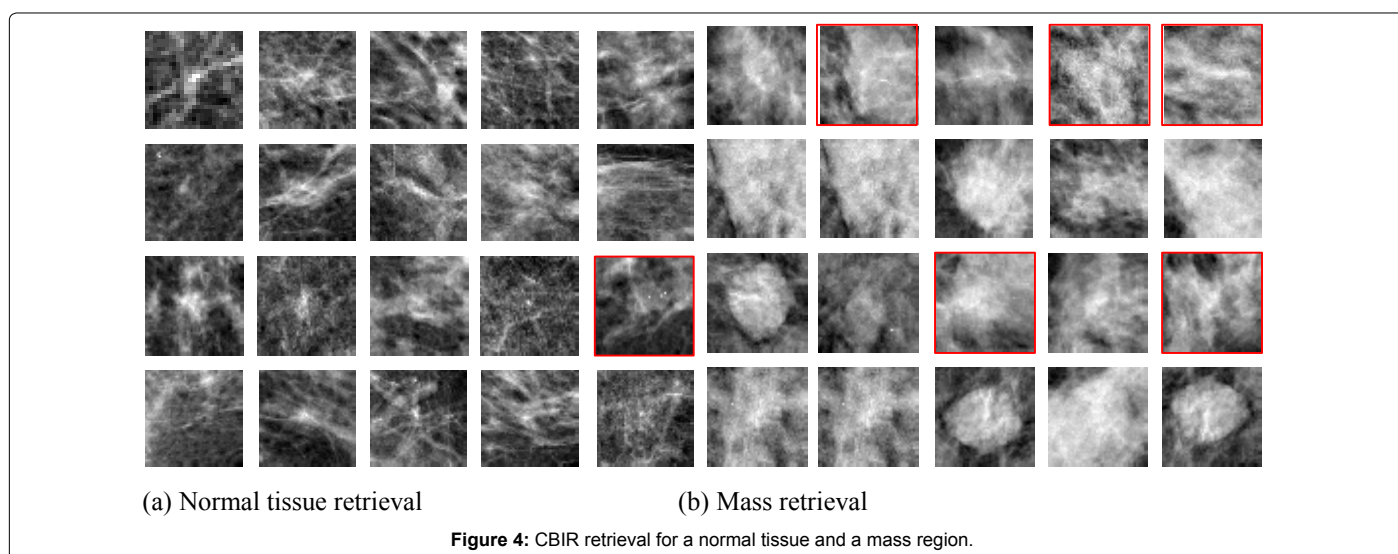vance, DAGH was put forward as a new representation [72]. Current CBIR systems analyze each view independently, a two-view CBIR system was proposed in Dhahbi et al. [73]. CBIR retrieval for a mass region and a normal tissue with [72] are shown in Figure 4. The left-top image is the query image. The remaining 19 images are the retrieval results. The query image in Figure 4(a) is a normal tissue. The query image in Figure 4(b) is a mass. The regions with red rectangle are the non-relevant images.

Discussion

For abnormalities detection, MC can get decent detection performance. However, the detection performance for mass is not satisfying. In previous studies, masses are detected using single view information. Recently, multi-view based detection draws more attention. For multi-view based detection, many problems are not well solved. As the breast is compressed during imaging, finding the corresponding regions in different views are not easy. The second problem is a good fusion strategy. Existing multi-view CAD normally employ two mammograms, ipsilateral mammograms or bilateral mammograms. Using four mammograms to detect simulates the radiologist's interpretation. Thus develop the four-view based CAD method is demanding. Another problem in existing CAD is the lack of fusing detection and CBIR. CBIR retrieves similar images from the database. How to effectively combine the retrieval results with the detection results can be studied. For abnormalities classification, the performance of existing methods still needs to be improved. Recently, deep learning methods have been applied to this topic and a good result was obtained. More researches for classification using deep learning may be another direction.

Conclusion

CAD can be served as a second view in the early detection of breast cancer. A large amount of work has been done in this field. This paper presented an overview of the recent development in CAD methods. Abnormalities detection, abnormalities classification and CBIR are briefly reviewed. Single-view based detection is the foundation of multi-view based detection and has been studied deeply. Multi-view based detection simulates the radiologist's interpretation. However, many problems including region matching and fusion strategy are not well solved. Another problem in existing CAD is the lack of fusing detection and CBIR. Besides, the performance of deep learning methods for abnormalities classification needs to be tested and improved.

(a) Normal tissue retrieval   (b) Mass retrieval

Figure 4: CBIR retrieval for a normal tissue and a mass region.

References

1. Ferlay J, Soerjomataram I, Ervik M (2013) Cancer incidence and mortality worldwide: IARC Cancer Base No. 11[M/OL]. Lyon: Agency for Research on Cancer.

2. Li Y, Chen H, Yang Y, Yang N (2013) Pectoral muscle segmentation in mammograms based on homogenous texture and intensity deviation. Journal Pattern Recognition 46: 681-691.

3. DeSantis C, Ma J, Bryan L, Jemal A (2014) Breast cancer statistics, 2013. CA Cancer J Clin 64: 52-62.

4. Howlander N, Noone AM, Krapcho M, Miller D, Bishop K, et al. (2014) SEER cancer statistics review, 1975–2011. Bethesda MD National Cancer Institute.

5. Chang Y, Hou-Jin C, Yong-Yi Y, Feng LY, Zhong HZ, et al. (2013) Microcalcification clusters processing in mammograms based on relevance vector machine with adaptive kernel learning. Acta Physica Sinica 62: 088702.

6. Tang J, Rangayyan RM, Xu J, EI Naqa I, Yang Y (2009) Computer-aided detection and diagnosis of breast cancer with mammography: recent advances. IEEE Trans Inf Technol Biomed 13: 236-251.

7. Nakayama R, Uchiyama Y, Yamamoto K, Watanabe R, Namba K (2006) Computer-aided diagnosis scheme using a filter bank for detection of microcalcification clusters in mammograms. IEEE Trans Biomed Eng 53: 273-283.

8. Kavitha K, Kumaravel N (2007) A Comparative Study of Various Micro Calcification Cluster Detection Methods in Digitized Mammograms. Systems, Signals and Image Processing, 2007 and 6th EURASIP Conference focused on Speech and Image Processing, Multimedia Communications and Services, pp: 405-409.

9. Halkiotis S, Botsis T, Rangoussi M (2007) Automatic detection of clustered microcalcifications in digital mammograms using mathematical morphology and neural networks. Signal Processing 87: 1559-1568.

10. Bhattacharya M, Das A (2007) Fuzzy logic based segmentation of microcalcification in breast using digital mammograms considering multiresolution. Machine Vision and Image Processing Conference, pp: 98-105.

11. Pal NR, Bhowmick B, Patel SK, Pal S, Das J, et al. (2008) A multi-stage neural network aided system for detection of microcalcifications in digitized mammograms. Neurocomputing 71: 2625-2634.

12. Oh WV, Kim KG, Kim YJ, Kang H, Ro J, et al. (2009) Detection of microcalcifications in digital mammograms using foveal method. Journal of Korean Society of Medical Informatics 15: 165-172.

13. Peng R, Chen H, Varshney PK (2009) Noise-enhanced detection of micro-calcifications in digital mammograms. IEEE Journal of Selected Topics in Signal Processing 3: 62-73.

14. Kalra PK, Kumar N (2010) A novel automatic microcalcification detection technique using Tsallis entropy & a type II fuzzy index. Journal of Computers & Mathematics with Applications 60: 2426-2432.

15. Harirchi F, Radparvar P, Moghaddam HA, Toosi KN, Dehghan F, et al. (2010) Two-level algorithm for MCs detection in mammograms using Diverse-Adaboost-SVM. Pattern Recognition (ICPR), 20th International Conference, pp: 269-272.

16. Oliver A, Torrent A, Lladó X, Tortajada M, Tortajada L, et al. (2012) Automatic microcalcification and cluster detection for digital and digitised mammograms. Knowledge-Based Systems 28: 68-75.

17. Zhang X, Gao X (2012) Twin support vector machines and subspace learning methods for microcalcification clusters detection. Engineering Applications of Artificial Intelligence 25: 1062-1072.

18. Zhang X, Homma N, Goto S, Kawasumi Y, Ishibashi T, et al. (2013) A Hybrid Image Filtering Method for Computer-Aided Detection of Microcalcification Clusters in Mammograms. J Med Eng 2013.

19. Zhang E, Wang F, Li Y, Bai X (2014) Automatic detection of microcalcifications using mathematical morphology and a support vector machine. Bio-medical Materials and Engineering 24: 53-59.

20. Petrosian A, Chan HP, Helvie MA, Goodsitt MM, Adler DD (1994) Computer-aided diagnosis in mammography: classification of mass and normal tissue by texture analysis. Phys Med Biol 39: 2273-2288.

21. Petrick N, Chan HP, Sahiner B, Arbor A, Wei D, et al. (1996) An adaptive density-weighted contrast enhancement filter for mammographic breast mass detection. Medical Imaging, IEEE Transactions 15: 59-67.

22. Campanini R, Dongiovanni D, Iampieri E, Lanconelli N, Masotti M, et al. (2004) A novel featureless approach to mass detection in digital mammograms based on support vector machines. Phys Med Biol 49: 961-975.

23. Cascio D, Fauci F, Magro R, Raso G (2006) Mammogram segmentation by contour searching and mass lesions classification with neural network. Nuclear Science, IEEE Transactions 53: 2827-2833.

24. Pereira RR Jr, Azevedo Marques PM, Honda MO, Kinoshita SK, Engelmann R, et al. (2007) Usefulness of texture analysis for computerized classification of breast lesions on mammograms. J Digit Imaging 20: 248-255.

25. Guo Q, Shao J, Ruiz VF (2009) Characterization and classification of tumor lesions using computerized fractal-based texture analysis and support vector machines in digital mammograms. International Journal of Computer Assisted Radiology and Surgery 4: 11-25.

26. Ke L, Mu N, Kang Y (2010) Mass computer-aided diagnosis method in mammogram based on texture features. Biomedical Engineering and Informatics (BMEI), 3rd International Conference 1: 354-357.

27. Giordano D, Kavasidis I, Spampinato C (2011) Adaptive local contrast enhancement combined with 2D discrete wavelet transform for mammographic mass detection and classification. Digital Information and Communication Technology and Its Applications. Springer Berlin Heidelberg, pp: 209-218.

28. Hussain M, Khan N (2012) Automatic mass detection in mammograms using multiscale spatial weber local descriptor. Systems, Signals and Image Processing (IWSSIP), 19th International Conference, pp: 288-291.

29. Gargouri N, Masmoudi DA, Masmoudi SD, Abid R (2012) A New GLLD Operator for Mass Detection in Digital Mammograms. Int J Biomed Imaging 2012.

30. Do Nascimento MZ, Martins AS, Neves LA, Pereira RR, Lúcia FE, et al. (2014) Classification of masses in mammographic image using wavelet domain features and polynomial classifier. Expert Systems with Applications 40: 6213-6221.

31. Tai SC, Chen ZS, Tsai WT (2014) An automatic mass detection system in mammograms based on complex texture features. IEEE J Biomed Health Inform 18: 618-627.

32. Sun X, Qian W, Song D (2004) Ipsilateral-mammogram computer-aided detection of breast cancer. Comput Med Imaging Graph 28: 151-158.

33. Sahiner B, Chan HP, Hadjiiski LM, Helvie MA, Paramagul C, et al. (2006) Joint two-view information for computerized detection of microcalcifications on mammograms. Med Phys 33: 2574-2585.

34. Van Engeland S, Karssemeijer N (2007) Combining Two Mammographic Projections In A Computer Aided Mass Detection Method. Med Phys 34: 898-905.

35. Wu YT, Wei J, Hadjiiski LM, Sahiner B, Zhou C, et al. (2007) Bilateral analysis based false positive reduction for computer-aided mass detection. Med Phys 34: 3334-3344.

36. Velikova M, Samulski M, Karssemeijer N (2008) Toward expert knowledge representation for automatic breast cancer detection. Artificial Intelligence: Methodology, Systems, and Applications. Springer Berlin Heidelberg, pp: 333-344.

37. Li M, Yajing S (2008) Detections of microcalcification clusters using multiple mammographic views. Bioinformatics and Biomedical Engineering, The 2nd International Conference, pp: 361-365.

38. Samulski M, Karssemeijer N (2011) Optimizing Case-based detection performance in a multiview CAD system for mammography. IEEE Trans Med Imaging 30: 1001-1009.

39. Tanner C, van Schie G, Lesniak JM, Karssemeijer N, Szekely G (2013) Improved location features for linkage of regions across ipsilateral mammograms. Med Image Anal 17: 1265-1272.

40. Ericeira DR, Silva AC, De Paiva AC, Gattass M (2013) Detection of masses based on asymmetric regions of digital bilateral mammograms using spatial description with variogram and cross-variogram functions. Computers in Biology and Medicine 43: 987-999.

41. Li Y, Chen H, Yang Y, Cheng L, Cao L (2015) A bilateral analysis scheme for false positive reduction in mammogram mass detection. Comput Biol Med 57: 84-95.

42. Wei J, Chan HP, Zhou C, Wu YT, Sahiner B, et al. (2011) Computer-aided detection of breast masses: four-view strategy for screening mammography. Med Phys 38: 1867-1876.

43. Singh S, Kumar V, Verma HK, Singh D (2006) SVM based system for classification of microcalcifications in digital mammograms. Conf Proc IEEE Eng Med Biol Soc 1: 4747-4750.

44. Karahaliou A, Boniatis I, Sakellaropoulos P (2007) Can texture of tissue surrounding microcalcifications in mammography be used for breast cancer diagnosis? Nuclear Instruments and Methods in Physics Research Section A: Accelerators, Spectrometers, Detectors and Associated Equipment 580: 1071-1074.

45. Verma B, Zhang P (2007) A novel neural-genetic algorithm to find the most significant combination of features in digital mammograms. Applied Soft Computing 7: 612-625.

46. Geetha K, Thanushkodi K, Kumar AK (2008) New particle swarm optimization for feature selection and classification of microcalcifications in mammograms. Signal Processing, Communications and Networking, International Conference, pp: 458-463.

47. Wei L, Yang Y, Nishikawa RM (2009) Microcalcification classification assisted by content-based image retrieval for breast cancer diagnosis. Pattern Recognition 42: 1126-1132.

48. Chen Z, Strange H, Denton E, Zwiggelaar R (2014) Analysis of mammographic microcalcification clusters using topological features. Breast Imaging. Springer International Publishing, pp: 620-627.

49. Raghavendra U, Acharya UR, Fujita H (2016) Application of Gabor wavelet and Locality Sensitive Discriminant Analysis for automated identification of breast cancer using digitized mammogram images. Applied Soft Computing 46: 151-161.

50. Rangayyan RM, El-Faramawy NM, Desautels JE, Alim OA (1997) Measures of acutance and shape for classification of breast tumors. IEEE Trans Med Imaging 16: 799-810.

51. Rangayyan RM, Mudigonda NR, Desautels JE (2000) Boundary modelling and shape analysis methods for classification of mammographic masses. Med Biol Eng Comput 38: 487-496.

52. Rangayyan RM, Nguyen TM (2007) Fractal analysis of contours of breast masses in mammograms. J Digit Imaging 20: 223-237.

53. Liu X, Li B, Liu J, Xin Xu, Feng Z (2012) Mass diagnosis in mammography with mutual information based feature selection and support vector machine. Intelligent Computing Theories and Applications. Springer Berlin Heidelberg, pp: 1-8.

54. Mudigonda NR, Rangayyan RM, Desautels JE (2000) Gradient and texture analysis for the classification of mammographic masses. IEEE Trans Med Imaging 19: 1032-1043.

55. Campos LFA, Silva AC, Barros AK (2005) Diagnosis of breast cancer in digital mammograms using independent component analysis and neural networks. Progress in Pattern Recognition, Image Analysis and Applications. Springer Berlin Heidelberg, pp: 460-469.

56. Rashed EA, Ismail IA, Zaki SI (2007) Multiresolution mammogram analysis in multilevel decomposition. Pattern Recognition Letters 28: 286-292.

57. Eltoukhy MMM, Faye I, Samir BB (2009) Using curvelet transform to detect breast cancer in digital mammogram. Signal Processing & Its Applications, 5th International Colloquium, pp: 340-345.

58. Jasmine JSL, Baskaran S, Govardhan A (2011) An automated mass classification system in digital mammograms using contourlet transform and support vector machine. International Journal of Computer Applications 31: 54-61.

59. Narvaez F, Romero E (2012) Breast mass classification using orthogonal moments. Breast Imaging. Springer Berlin Heidelberg, pp: 64-71.

60. Nanni L, Brahnam S, Lumini A (2012) A very high performing system to discriminate tissues in mammograms as benign and malignant. Expert Systems with Applications 39: 1968-1971.

61. Li Y, Chen H, Rohde GK, Yao C, Cheng L, et al. (2015) Texton analysis for mass classification in mammograms. Pattern Recognition Letters 52: 87-93.

62. Mu T, Nandi AK, Rangayyan RM (2008) Classification of breast masses using selected shape, edge-sharpness, and texture features with linear and kernel-based classifiers. J Digit Imaging 21: 153-169.

63. Rouhi R, Jafari M, Kasaei S, Keshavarzian P (2015) Benign and malignant breast tumors classification based on region growing and CNN segmentation. Expert Systems with Applications 42: 990-1002.

64. Wei CH, Li Y, Li CT (2007) Effective extraction of Gabor features for adaptive mammogram retrieval. Entropy 2: 1503-1506.

65. Wei L, Yang Y, Wernick MN, Nishikawa RM (2009) Learning of perceptual similarity from expert readers for mammogram retrieval. Selected Topics in Signal Processing, IEEE Journal of Selected Topics in Signal Processing 3: 53-61.

66. Alto H, Rangayyan RM, Desautels JEL (2005) Content-based retrieval and analysis of mammographic masses. Journal of Electronic Imaging 14: 1-17.

67. Li Y, Wei CH (2011) Hierarchical correlation for content-based image retrieval. Multimedia Technology (ICMT) International Conference, pp: 550-553.

68. Siyahjani F, Ghaffari A, Fatemizadeh E (2011) Mammogram image retrieval via sparse representation. Biomedical Engineering (MECBME), 2011 1st Middle East Conference, pp: 63-66.

69. Tourassi GD, Harrawood B, Singh S, Lo JY, Floyd CE (2007) Evaluation of information-theoretic similarity measures for content-based retrieval and detection of masses in mammograms. Med Phys 34: 140-150.

70. Lu P, Liu W, Xu W, Li L, Zheng B, et al. (2012) Multi-instance learning for mass retrieval in digitized mammograms. SPIE Medical Imaging. International Society for Optics and Photonics, pp: 1-8.

71. Liu J, Zhang S, Liu W, Zhang X, Metaxas DN, et al. (2014) Scalable mammogram retrieval using anchor graph hashing. Biomedical Imaging (ISBI), IEEE 11th International Symposium, pp: 898-901.

72. Li Y, Chen H, Cao L, Zhong HZ, Lin C, et al. (2014) Mass retrieval in mammogram based on hashing theory and linear neighborhood propagation. Acta Phys Sin.

73. Dhahbi S, Barhoumi W, Zagrouba E (2015) Multi-view score fusion for content-based mammogram retrieval. Eighth International Conference on Machine Vision. International Society for Optics and Photonics.